REPORT TO THE

NATIONAL AERONAUTICS AND SPACE ADMINISTRATION

SEMIANNUAL STATUS REPORT #7

for

GRANT NAG 5-1490

INVESTIGATION OF PASSIVE ATMOSPHERIC SOUNDING USING MILLIMETER AND SUBMILLIMETER WAVELENGTH CHANNELS

A.J. Gasiewski (Principal Investigator)

D.B. Kunkee (Graduate Student)
D.M. Jackson (Graduate Student)
W. Blackwell (Undergraduate Student)
S. Sharpe (Undergraduate Student)

Covering the period from

January 1, 1994 to June 30, 1994

Submitted by:

Professor Albin J. Gasiewski
School of Electrical Engineering
Georgia Institute of Technology
Atlanta, Georgia, 30332-0250
(404) 894-2934

NASA Technical Officer:

Dr. Robert F. Adler
Laboratory for Atmospheres/Code 612
NASA Goddard Space Flight Center
Greenbelt, MD 20771
(301) 286-9086

TABLE OF CONTENTS

INTRODUCTION

Progress by the Georgia Institute of Technology's Laboratory for Radioscience and Remote Sensing in developing techniques for passive microwave retrieval of water vapor profiles and cloud and precipitation parameters using millimeter- and sub-millimeter wavelength channels is reviewed. Channels of particular interest are in the tropospheric transmission windows at 90, 166, 220, 340 and 410 GHz and centered around the water vapor lines at 183 and 325 GHz. Collectively, these channels have potential application in high-resolution precipitation mapping (e.g., from geosynchronous orbit), remote sensing of cloud and precipitation parameters, including cirrus ice mass, and improved retrieval of water vapor profiles.

During the period from January 1, 1994 through June 30, 1994 research activities focussed on calibrating and interpreting data from the Millimeter-Wave Imaging Radiometer (MIR). The MIR was deployed on the NASA ER-2 during the Convective Atmospheric Moisture Experiment (CAMEX, September-October 1993) to obtain the first submillimeter-wave tropospheric imagery of convective precipitation. A 325-GHz radiometer consisted of a submillimeter-wave DSB receiver with three IF channels at +/-1,3, and 8.5 GHz, and ~14 dB DSB noise figure was successfully operated during these experiments. Activities supported under this grant include a study of the impact of local oscillator reflections from the MIR calibration loads, the development of optimal gain and offset filters for radiometric calibration, and the modelling and interpretation of the MIR 325-GHz data over both clear and cloudy atmospheres. In addition, polarimetric radiometer measurements and modelling for ocean surface and atmospheric cloud-ice studies were supported.

DISCUSSION OF ACTIVITIES

Activities within the period from July 1, 1993 through December 31, 1993 under NASA grant NAG 5-1490 have focused primarily on the calibration of and interpretation of radiometric imagery obtained using the Millimeter-wave Imaging Radiometer (MIR) instrument. The MIR is a cross-track scanning imaging radiometer with channels at 89, 150, 183+/-1,3,7, 220, and 325+/-1,3,8 GHz. The MIR was successfully flown on the high-altitude NASA ER-2 platform during several deployments, including TOGA/COARE (January-February, 1993) and CAMEX (September-October 1993). During the CAMEX deployment the three channels near the 325-GHz submillimeter-wave water vapor line were operative, providing the first submillimeter-wave imagery of tropospheric clouds and precipitation as observed from a downward-looking perspective.

Specific activities involving the MIR have included: (1) interpretation of the first wideband MIR imagery over clear-air, clouds, and convective precipitation, (2) determination of the effects of local oscillator reflection from MIR calibration loads and characterization of the passband response of the MIR, (3) determination of the optimum shape and width of gain and offset filters for optimal radiometer calibration, (4) refinement of comparisons of clear-air MIR brightness measurements with calculations based on water vapor profiles derived from coincident raobs and Raman lidar water vapor profiles. Additional related activities include studies of dual-polarization radiometer signatures of both precipitation cell tops and anisotropic ocean features observed during TOGA/COARE.

The MIR is a joint project between the NASA Goddard Space Flight Center and the Laboratory for Radioscience and Remote Sensing at Georgia Tech. Past Georgia Tech contributions to the MIR and its related scientific uses have included basic system design studies, performance analyses, circuit and radiometric load design, in-flight software, provision of the 325-GHz receiver, operation of the MIR during field deployments, development of post-flight data display and calibration software, and radiative transfer studies of the effects of clouds, water vapor, and precipitation on MIR brightness temperatures. From December 1993 through May 1994 the MIR was

moved to Georgia Tech for characterization and ground-based experiments involving the 325-GHz radiometer.

1. Wideband MIR Imagery

Nine-channel MIR imagery covering the bands 89 through 325 GHz observed on several ER-2 flights during TOGA/COARE and CAMEX has been displayed and is undergoing preliminary analysis. An example of this imagery obtained during overflights of oceanic convection on September 27, 1994 is shown in Figure 1. Studies of this and several similar data sets indicate that the 325-GHz channels will be useful for mapping raincells, measuring cirrus ice content, and enhanced detection of clouds for the purpose of improving water vapor soundings.[1] In addition, significantly higher spatial resolutions can be achieved using these channels instead of (or, in conjunction with) conventional rain mapping microwave channels at 19, 37 or 89 GHz.

A statistical analyses of the window channel data (89, 150, 220, and 325+/-8 GHz) show at least two significant spectral modes observed over raincells. The method of empirical orthogonal eigenfunctions was used for this analysis. These most dominant mode was found to represent a decrease in the brightness temperature of all four channels. This decrease is comparable among all four channels and is the result of strong ice scattering of the cold cosmic background. The contribution to this mode at 325+/-8 GHz can be expected by extrapolation of the response to ice seen at 89, 150, and 220 GHz.

The second- and third-order modes are most closely related to the slope and curvature (respectively) of the brightness spectrum sampled at these window channels. In particular, the second mode is correlated with radiometrically thin portions of raincells, for example, anvil regions. Although a complete geophysical interpretation of these modes is not yet available, their large signal-to-noise ratios (each greater than 10 dB each) suggest that useful precipitation cell characteristics can ultimately

---

[1] Support for these conclusions is provided in the attached conference publication "Airborne Imaging of Tropospheric Emission at Millimeter and Submillimeter Wavelengths," by Gasiewski et al, accepted for presentation at the 1994 International Geoscience and Remote Sensing Symposium [Appendix A].

be derived from them.

One feature of the 325 GHz imagery that had not been anticipated is the flatness of the clear-air spectra near the 325-GHz line. Clear-air radiative transfer calculations based on the Liebe model [1985] show brightness temperatures that are distinctly colder near the line center (325 +/-1 GHz) than near the line wings (+/-8 GHz). The model calculations were for US standard atmospheric temperature conditions and for widely varying humidity conditions. For example, in the dry extreme the humidity profile was chosen to be exponentially decaying with 2-km scale height and a relative humidity of 20% at the surface; in the moist extreme the relative humidity at the surface was 100%. These resulting brightness differences between 325+/-8 GHz and 325+/-1 GHz channels were predicted to be between 21 and 27 K [Gasiewski 1992], and comparable to that predicted (and observed) near the 183-GHz line [Jackson and Gasiewski 1994].

However, the clear-air MIR data over similar temperature conditions show much less of a difference between the line center and wing brightness temperatures. Observed differences between the 325+/-8 and 325+/-1 channels are typically no greater than 5-6 K for the prevailing conditions during CAMEX. Although it has not yet been ascertained that the air was clear by optical means, is has been ascertained using passive infared data from the High-resolution Infrared Sounder that cloud cover was perhaps broken for some of the imagery, but certainly not solid for the entire set of CAMEX flights. Lab experiments by both Georgia Tech and the receiver manufacturer (ZAX MMW Corporation) have been used to rule out local oscillator drift as a possible cause of this anomoly. Moreover, the varying degree of ice scattering exhibited by the cell-top imagery at the three 325-GHz channels verifies that the local oscillator was centered on the 325.153-GHz H_2O line to within an acceptable margin of error.

However, it cannot be ruled out that the 325 GHz receiver was not responding to a subharmonic RF band during CAMEX, for example, near 243.86 GHz. The 325 GHz receiver on the MIR has an overmoded input waveguide that allows passage of signals down to about 200 GHz or so. Since the mixer is driven subharmonically at one-fourth of the 325-GHz RF frequency there are necessarily current harmonics at three-fourths of the RF frequency, or 243.865 GHz, present in the mixer. The effects of reflections at this

frequency from metal plates in front of the 325 GHz feedhorn have, in fact, been observed. Thus, it is possible that the 325 GHz channels might actually have been receiving a mix of data from 325.153+/-1,3,8 and 243.865+/-1,3,8 GHz channels. This could account for the "flatness" of the clear-air brightness spectrum across the 325-GHz channels. In other words, the spectrum around 243.865 GHz (which is indeed quite flat) could be being added to the spectrum around 325.153 GHz. Of course, under this scenario some 325 GHz spectral structure over stormcells would still appear, as has been seen in the data.

2. Local Oscillator Reflection Tests

As an important step in improving and verifying the absolute calibration of the MIR we have performed local oscillator (LO) reflection measurements using both metallic and absorbing reflectors. The measurements took place at Georgia Tech during the winter of 1994. The LO reflection test configuration consists of the MIR with its antennas trained on a perfectly- or partly-reflecting surface. Any leakage of LO signals from the RF ports of the mixers is reflected back into the instrument. By moving the surface along the antenna beam axis the phase of the reflected signal can be varied over a complete cycle. The impact of LO reflections via the RF ports of the mixers can be diagnosed by measuring the MIR video output signal at several positions of the surface. A Fourier transform of the measured data as a function of surface position shows the relative effect of all harmonics of the LO frequency on the radiometer output. In effect, a simple Fourier-transform spectrometer was implemented.

To perform the LO tests a computer-controlled mechanical translator was configured to step the reflecting surfaces over a 3-cm range in 10 micron increments. Video voltage samples were recorded at each step. Surfaces included both a flat aluminum plate and a styrofoam-covered pyramidal absorbing load. The absorbing load was identical to those used to calibrate the MIR.

Voltage spectra for both an aluminum plate and pyramidal load are displayed in Figures 2a and b. Using the aluminum plate the video output was seen to vary over a range equivalent to 85 K and harmonics of the LO up to 8th order were evident (Figure 2a). Although the pyramidal load reduces the level of reflection there is still a residual peak-to-peak variation of

1.5 K caused by the LO fundamental signal at 150 GHz (Figure 2b). Since a similar variation can occur each time the MIR observes a calibration load it is thought that LO reflection is a major cause of bias in the 150 GHz channel. Such a calibration bias could easily explain inaccuracies in brightness temperature observed over LN_2 targets. However, only the 150-GHz channel exhibits adverse LO reflection behavior; all other channels exhibit negligible output variations under the LO reflection test when the pyramidal load is used.

3. MIR Calibration

In order to accommodate the relatively large noise levels of the 325-GHz channels, as well as to improve the calibration of the other channels, a nonlinear calibration filter is being developed. The filter is based on: (1) identification and removal of non-stationary features in the single-scan gain and offset data, (2) subsequent optimal time-invariant filtering of the residual gain and offset signals, and (3) reconstruction of the overall gain and offset waveforms. The non-stationary features include jumps and spurious noise. An iterative technique based on the CLEAN algorithm is used for detection of these features. Upon removal, an time-invariant linear filter is constructed for each radiometric channel for both the gain and offset processes. The filters are based on the estimated noise levels and autocorrelation time constants for the particular channel [Adelberg et al., 1993]. In this manner, the unique statistical characteristics of each channel are accommodated.

By varying the width of the gain and offset filters the standard deviation of noise resulting from calibration errors can be minimized. This was investigated by implementing a triangular gain and offset calibration filters of varying widths, then computing the resulting error. The results (Figure 3) show that the optimal filter width can vary greatly provided that the widths of the gain and offset filters are nearly the same. The requirement of similarity between the gain and offset filters appears to be a general result, irrespective of the statistics of the particular radiometer. The application of an optimal calibration algorithm, accommodation of the new 325-GHz channels, and the provision of several new data editing features required major modifications to the post-flight data analysis software. Some of these have been incorporated into a new MIR

image analysis program which uses disk-based storage of the imagery. The PC-compatible software will also incorporate a variety of simple interactive features for MIR data analysis. The MIR data is also being archived on 35-mm slides for graphical storage and dissemination.

4. Clear-Air MIR Brightness Comparisons

Detailed comparisons of observed brightness temperatures using the MIR data and brightness temperature calculations based on coincident radiosonde and Raman lidar data have been performed at Georgia Tech. Both airborne and ground-based observations were considered in the study. The results of the study are described by Jackson and Gasiewski [1994].[2] During a review of the study it was discovered that the GSFC Raman lidar humidity profiles were positively biased between 8 and 10 km, necessitating recalculation of the brightness values. Hence, in the published comparisons only lidar humidity values up to 8 km are used. The overall conclusions of the study are that (1) the Liebe model for absorption near 183 GHz is acceptable to within the combined measurement errors of the instruments used in the comparison, (2) the lidar data up to approximately 8 km are consistent with MIR observations, and (3) the AIR-type radiosondes report excessive moisture in the upper troposphere. The Vaisala-type radiosondes provide the best consistent with the MIR observations.

While water vapor absorption is well-understood near 183 GHz, the MIR CAMEX brightness temperatures and ground-based observations performed at Georgia Tech during January-February 1994 show significant discrepancies with calculated brightness temperatures for the 325 GHz channels. However, the comparisons were made using either standard atmosphere models or soundings that were not well collocated with the radiometer measurements Thus, these comparisons are not readily interpretable. A more extensive set of airborne- and ground-based experiments to determine the accuracy of the prevailing absorption model at 325 GHz is needed.

---

2 "Millimeter-Wave Radiometric Observations of the Troposphere: A Comparison of Measurements and Calculations Based on Radiosonde and Raman Lidar," accepted for publication in the IEEE Transactions on Geoscience and Remote Sensing, July, 1994.

5. Polarimetric Microwave Radiometry

It is hypothesized that polarimetric microwave radiometry can be used for spaceborne remote sensing of ocean wave direction [Wentz, 1992; Dzura 1992] and for detection of oriented thunderstorm anvil ice [Evans and Vivekanandan, 1990]. We have investigated the former hypothesis both experimentally and theoretically using fully polarimetric laboratory measurements at 92 GHz of upwelling emission from a fresh-water wave tank [Gasiewski and Kunkee, 1994]. The wave tank measurements are well corroborated by a geometrical optics emission model for anisotropic surfaces (Figures 4-7). Both the model and measurements show that significant brightness variations in the first three Stokes parameters can be produced by only moderately striated dielectric surfaces. The data account for small random angular variations of the direction of the waves within the tank.

Specifically, the laboratory measurements show a predictable dependence of $T_U=\mathrm{Re}\langle E_v E_h^* \rangle$ on the direction of the water wave, with peak-to-peak amplitudes of up to 20 K at steep observation angles (Figure 7). An interesting phase reversal (along with corresponding amplitude null) occurs in the second Fourier azimuthal harmonic for observations near 40^o from zenith (Figure 5). The T_U angular variations are in phase quadrature with the variations exhibited by T_v and T_h, suggesting that passive remote sensing of surface wave direction can be facilitated by polarimetric microwave radiometry. Both the measurements and model calculations consider all four Stokes' parameters, although the last of these ($T_V=\mathrm{Im}\langle E_v E_h^* \rangle$) is very small and not expected to be useful for geophysical remote sensing of the troposphere or surface.

The encouraging results of the wave tank experiment prompted an airborne field experiment during TOGA/COARE to investigate passive polarimetric measurement of ocean wave direction. Indirectly, one can be expected to infer atmospheric wind direction from such measurements. Electronic and hardware modifications necessary to operate the polarimetric radiometer on the NASA DC-8 aircraft were performed. A total of twenty DC-8 flights occurred during TOGA/COARE, including seven low-altitude (1.5-4 km) constant bank-angle maneuvers designed to provide views of the ocean

surface at a constant observation angle and over a range of azimuthal angles [Kunkee and Gasiewski, 1994, Appendix B].

Post-mission calibration of nearly all of the 92-GHz polarimetric data has been completed [See Appendix C, TOGA/COARE AMMR 92 Data Processing]. A plot of the constant bank-angle data for an incidence angle of 65° (Figure 8) shows residual peak-to-peak brightness variations over azimuthal angle of amplitude ~3 K for T_v and T_h. The shape and amplitude of the azimuthal variations are similar to those found by Wentz. Even for observation at nadir, sinusoidal brightness variations of amplitude ~1.K (complementary in T_v and T_h) can be seen. Although the nadir variations are not large enough for retrieval purposes, they are large enough to adversely impact brightness measurements for some atmospheric sounding purposes, for example, wet path delay measurements or water vapor sounding.

Recently, we have extended our anisotropic surface model to accommodate realistic wind-driven ocean surfaces. A Monte-Carlo model of surface emission using geometrical optics with multiple scattering was developed for this purpose. The model incorporates a standard ocean wave amplitude spectrum with a prescribe phase spectrum. The incorporation of a phase spectrum into the ocean surface realization is unique and represents a new contribution to statistical ocean surface modelling. An ocean foam distribution appropriate for wind-driven waves is also incorporated. The foam model produces larger amounts of foam on the leeward sides of waves than on the windward side. The addition phase and foam to the standard ocean surface model has resulted in computed azimuthal brightness variations that well corroborate the wind-dependent brightness variations published by Wentz (Figures 9a and b).

In addition to striated water surfaces, it has been hypothesized that polarimetric microwave signatures in T_v, T_h, and T_U will be produced by oriented ice particles, for example, in electrified cirrus anvils. For example, microwave depolarization signatures in space-to-ground communications links have been associated with lightning discharges [Cox and Arnold, 1979]. Calibrated 92-GHz polarimetric data observed over an oceanic storm during TOGA/COARE on February 4, 1993 (Figure 10) are believed to show such variations. Over the most radiometrically cold part of the storm a rapid change in polarization of almost 12 K is observed. The

distance over which the change occurs is approximately 12 km. The cold brightness temperatures both within and adjacent to the storm center suggest that the mechanism responsible for the change must be ice scattering. Ocean surface variations (which might change the polarization difference) would not be visible through the highly-opaque storm. Supporting data from the other side-looking radiometric instruments that flew on the DC-8 is being sought to further investigate this case.

6. Digital Correlator for Polarimetric Radiometry

In anticipation of the need for precision airborne and spaceborne polarimetric radiometry, a high-speed digital correlator for proposed use in the NASA/MSFC Advanced Microwave Precipitation Radiometer (AMPR) is being developed.[3] A prototype A/D converter operating at 1000 Ms/sec and using standard emitter-coupled logic (ECL) has been demonstrated. Two such A/D converters along with three high speed (1000 MHz) digital counters are the essential components of the correlator. The reason for using digital correlation is that calibration of the cross-correlation channel can be accurately performed using only the standard hot and cold calibration targets found in convectional radiometers. The performance of our prototype converter suggests that the necessarily wide IF bandwidths required for Earth remote sensing (in this case, up to 500 MHz) can be obtained using the digital technique. Development of a complete 500 MHz breadboard unit for demonstration purposes is in progress.

---

[3] A proposal for much more extensive development of digital correlation polarimetry and its evaluation on the NASA/MSFC AMPR has been submitted by this PI to NASA Headquarters under the title "Passive Measurement and Interpretation of Polarized Microwave Brightness Temperatures," September 1992, NASA control # 2916-RD-074.

SUMMARY AND PLANS FOR FUTURE WORK

The investigations conducted over the past six months have served several purposes, including: (1) the first demonstration of radiometric imaging for meteorological purposes at 325 GHz, (2) the development and implementation of optimal techniques for radiometer calibration, (3) identification of the number of observable degrees of freedom in wideband 90, 150, 220, and 325+/-8 GHz imagery of stormcells, (4) the identification of a possible clear-air brightness temperature anomoly at 325 GHz, (5) corroboration of brightness temperature anisotropies at 92 GHz produced by both controlled waves and ocean waves at 92 GHz, (6) identification of a polarization difference signature observed over convection, and (7) demonstration of the essential electronic components for a digital correlator for precision polarimetric radiometry. Future plans which build on the findings of these investigations are outlined below.

1. MIR Observations and Data Analysis

Several convective case studies from CAMEX are being compiled for statistical analysis. During the convective overflight on October 5, 1993, the ER-2 Doppler radar (EDOP) obtained coincident nadir reflectivity profiles. This is the first joint EDOP and MIR data set. Because of the coincident EDOP radar truth, analysis of the MIR data from this flight is of great interest.

Two of the MIR case studies identified during TOGA/COARE are particularly interesting for radiative transfer experiments, namely, the overflights of cyclone Oliver and the Kavieng ground observation site. To this end, we plan to simulate ocean surface and atmospheric conditions within the eye of cyclone Oliver to determine the consistency of wideband radiative transfer models using the observed brightness data. The radiative transfer model will consider the effects of increasing humidity, precipitation, and ocean roughness near the eyewall to determine the relative contributions of these components to the warm ring.

The Kavieng overflights will be used to provide data for simulating the effects of clouds on upwelling MMW brightness temperatures. Ground-based radiometer data will be used to determine total water vapor and cloud

content, while ground-based lidar will be used to determine cloud bottom altitudes. Radiosondes will be further used to constrain the vertical distribution of water vapor. Of interest is a comparison of computed and observed upwelling brightness temperature, and in particular, the impact that clouds have on these temperatures.

To further investigate the wideband imaging capabilities of the MIR, images of Oliver from TOGA/COARE and convective precipitation from CAMEX using the AMPR, MIR, and MTS are being compiled. The data will be useful for wideband RT modelling and precipitation structure studies. The analysis of Oliver will require some data from the JPL ARMAR; this is available and being requested.[4]

The 325-GHz clear-air brightness discrepancies are, if spectroscopic in nature, extremely interesting. Accordingly, we plan further studies to determine whether the discrepancies could be instrumental, or whether they can be explained by minor reductions to the 325.153 GHz line strength and/or increases in the H_2O continuum absorption near the line wings. RF response measurements at 243.865 and 325.153 GHz will be attempted to determine if the lower of these bands is indeed being received. Very little power needs to be leaked into the antenna at these frequencies to determine this. If RF response at 243.865 GHz is found to occur a high-pass filter will be designed for installation into the 325 GHz RF path. If the lower band is indeed being received, a determination of the approximate radiometric response of this band relative to the 325-GHz band will be attempted. Knowing the relative responses of these bands will allow the CAMEX data to be interpreted properly.

If the absence of instrumental errors, additional aircraft observations over Raman lidar and/or raob sites, and under colder prevailing temperature conditions would be needed to more completely determine modifications to the Liebe model. Accordingly, the PI plans to work with investigators at NASA/GSFC to organize an appropriate field experiment for this purpose. A ground-based field experiment performed in conjunction with other ground-based profiling instruments operated by the NOAA Environmental Research

---

[4] Collaborating on the TOGA/COARE data analysis is Dr. J. Vivekanandan of the University of Colorado.

Laboratory (ERL) in Boulder, CO will be organized. The experiments will be planned for winter and spring of 1995.

2. Radiometer Calibration

These simple LO reflection measurements will provide answers to questions concerning the absolute calibration of the MIR and the use of the 183 and 325-GHz data in radiative transfer intercomparisons. Documentation of the LO reflection experiments will be performed during the next two quarters. Particular attention is being paid to the 150 GHz channel, which consistently returns brightness temperatures that are 5-10 K colder than expected from an absorber immersed in liquid nitrogen.

The nonlinear optimal calibration technique is nearly ready for operational calibration of all MIR data, including flights during CAMEX and TOGA/COARE. During the next two quarters we plan to archive the calibrated data so that it will be available to investigators collaborating on TOGA/COARE studies. A 1-GB hard disk drive has been obtained under this grant to support the calibration and archival effort.

Accurate absolute calibration of the MIR (and similar radiometers) requires that the total reflectivity of the hot and cold loads be less than ~1%, and known to better than 0.1%. Manufacturer's specifications typically provide only the specular component of the reflectivity, which is thought to be substantially less than the total reflectivity. In order to refine the MIR calibration, we plan to extend the study of the electromagnetic scattering and absorption characteristics of wedge-type blackbody loads to the more desirable pyramidal loads. The electromagnetic scattering analysis should be useful in the design of wideband calibration loads for radiometers, and specifically, for determining the reason for the enhanced LO reflection sensitivity of the MIR's 150 GHz channel.

Our approach is to develop numerical models for one- and two-dimensionally periodic lossy gratings using the coupled wave method. We currently have software based on the coupled wave method to predict the reflectivity of one-dimensionally periodic loads of arbitrary dielectric profile. Extension of the coupled wave model to two-dimensionally periodic surfaces appears feasible, and will be continued. In addition to the electromagnetic analysis, work on the steady state thermal analysis for two-dimensionally periodic calibration loads will be continued. Although,

the radiometric calibration load reflectivity analysis is of importance in understanding precision radiometer calibration, it is of secondary importance relative to the MMW and SMMW data analysis.

3. Polarimetric Radiometry

It is expected that future activities regarding the investigation of polarimetric passive remote sensing will be supported under a separate grant from NASA Headquarters. These activities include the development of digital correlation hardware for upgrading the NASA/MSFC Advanced Microwave Precipitation Radiometer (AMPR) for fully polarimetric imaging capability. The bandwidth of the correlator will be approximately 500 MHz. The upgraded AMPR will be useful for wideband radiometric studies of both the ocean surface and precipitating atmospheric convection.

As part of the polarimetric remote sensing study, the NASA/GSFC 92-GHz polarimetric radiometer will be used for testing and evaluation purposes. Provisions for the extended loan of this instrument at Georgia Tech will be made. Several suggestions for upgrading the GSFC 92-GHz polarimetric radiometer have been identified, and are presented in Appendix D.

REFERENCES

Adelberg, L.K., A.J. Gasiewski and D.M. Jackson, "Optimal Calibration of Radiometers using Discrete Wiener Filters", presented at the 1993 International Geoscience and Remote Sensing Symposium, Tokyo, Japan, August 18-23, 1993.

Cox, D.C., and H.W. Arnold, "Observations of Rapid Changes in the Orientation and Degree of Alignment of Ice Particles Along an Earth-Space Radio Propagation Path", J. Geophys. Res., vol. 84, pp. 5003-5010, 1979.

Dzura, M.S., V.S. Etkin, A.S. Khrupin, M.N. Pospelov, M.D. Raev, "Radiometers-Polarimeters: Principles of Design and Applications for Sea Surface Microwave Emission Polarimetry", Proceedings of the 1992 IEEE International Geoscience and Remote Sensing Symposium (IGARSS), pp. 1432-1434, June, 1992.

Evans, K.F., and J. Vivekanandan, "Multiparameter Radar and Microwave Radiative Transfer Modeling of Nonspherical Atmospheric Ice Particles", IEEE Trans. Geosci. Remote Sensing, Vol. 28, No. 4, pp. 423-427, July, 1990.

Gasiewski, A.J., "Numerical Sensitivity Analysis of Passive EHF and SMMW Channels to Tropospheric Water Vapor, Clouds, and Precipitation", IEEE Trans. Geosci. Remote Sensing, Vol. 30, No. 5, pp. 859-870, September, 1992.

Gasiewski, A.J., and D.B. Kunkee, "Microwave Thermal Emission from Water Waves", accepted for publication in Radio Science, July, 1994.

Jackson, D.M., and Gasiewski, A.J., "Millimeter-Wave Radiometric Observations of the Troposphere: A Comparison of Measurements and Calculations Based on Radiosonde and Raman Lidar," accepted for publication in IEEE Transactions on Geoscience and Remote Sensing, July, 1994.

Kunkee, D.B., and A.J. Gasiewski, "Airborne Passive Polarimetric Measurements of Sea Surface Anisotropy at 92 GHz," Proceedings of the 1994 International Geoscience and Remote Sensing Symposium (IGARSS), presented at the California Institute of Technology, Pasadena, CA, August 8-12, 1994.

Liebe, H.J., "An Updated Model for Millimeter-Wave Propagation in Moist Air", Radio Sci., Vol. 20, No. 5, pp. 1069-1089, 1985.

Wentz, F.J., "Measurement of Oceanic Wind Vector Using Satellite Microwave Radiometers", IEEE Trans. Geosci. Remote Sensing, vol. 30, no. 5, pp. 960-972, September 1992.

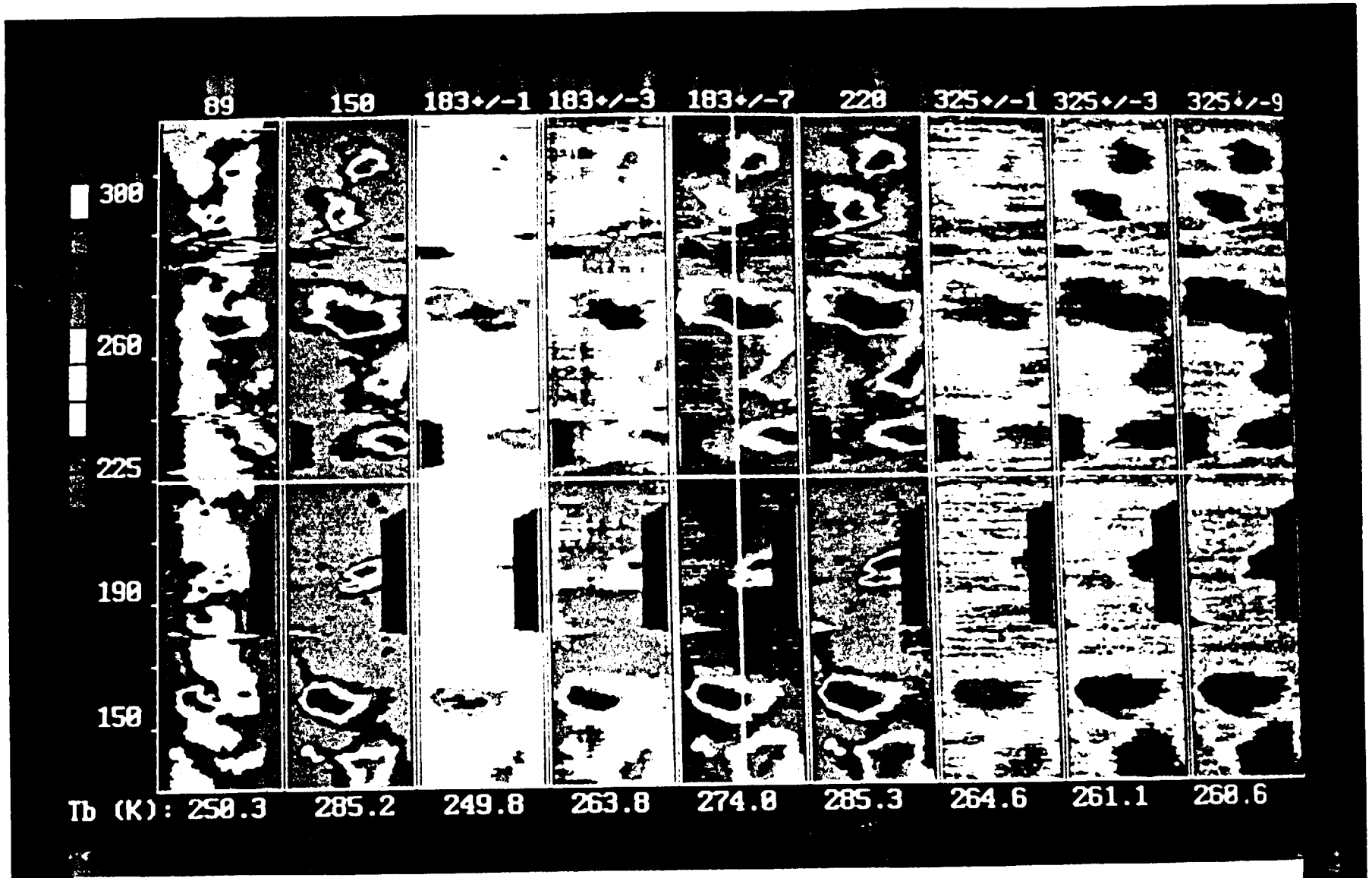

Figure 1. Strip-map images of upwelling thermal emission from isolated oceanic convective cells (September 27, 1994). Each map covers approximately 40 x 220 km; cells are distorted slightly due to their proximity to the aircraft. Average clear-air brightness temperature values at nadir are indicated below each map.

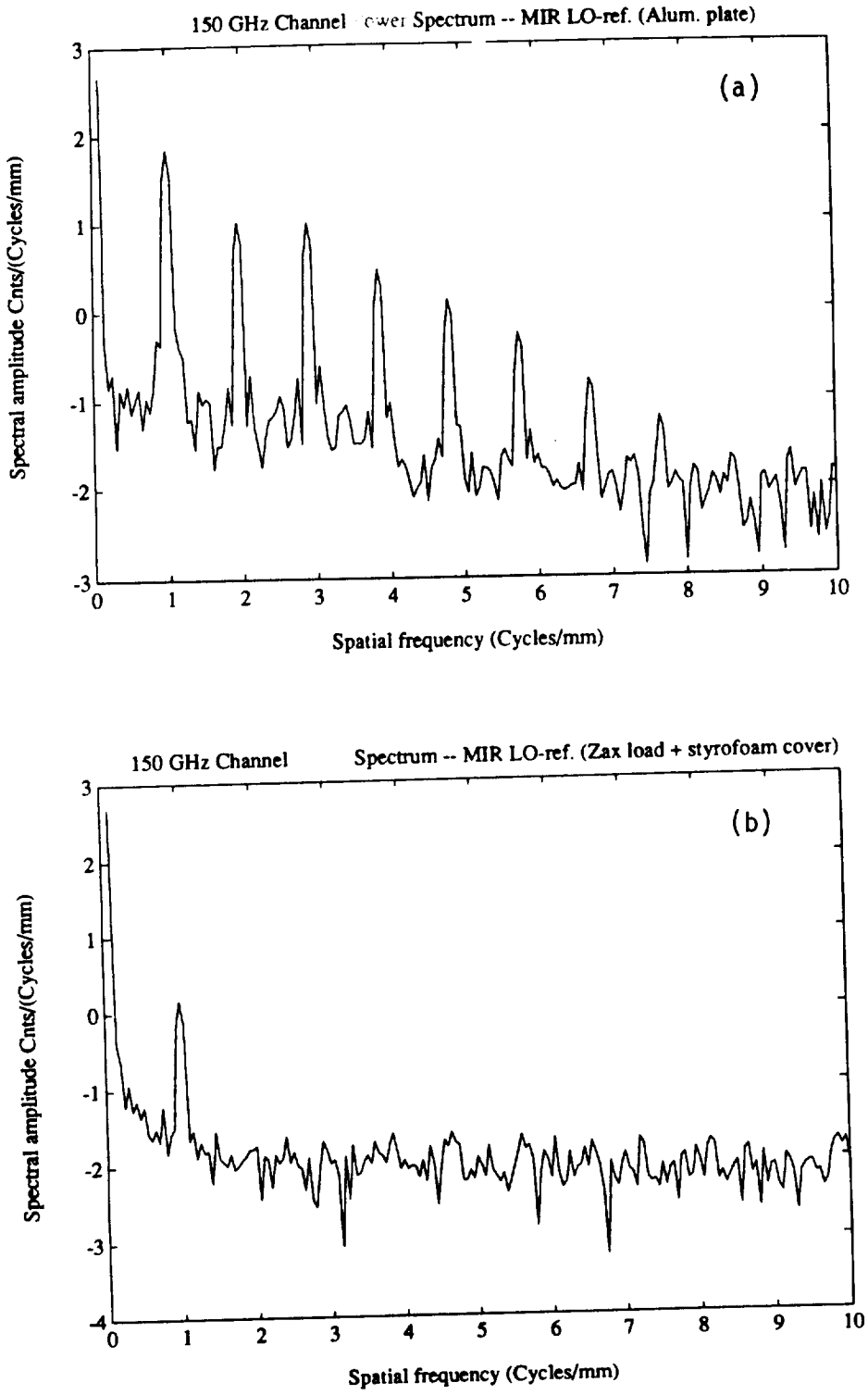

Figure 2. Video voltage spectra of the MIR 150-GHz channel as a function of spatial frequency for LO reflection tests using (a) flat aluminum plate, and (b) pyramidal calibration load. Reflections at harmonics of the 150 GHz LO signal are indicated by the equally-spaced peaks. The vertical scale is in deciBels/10; the reference level is arbitrary.

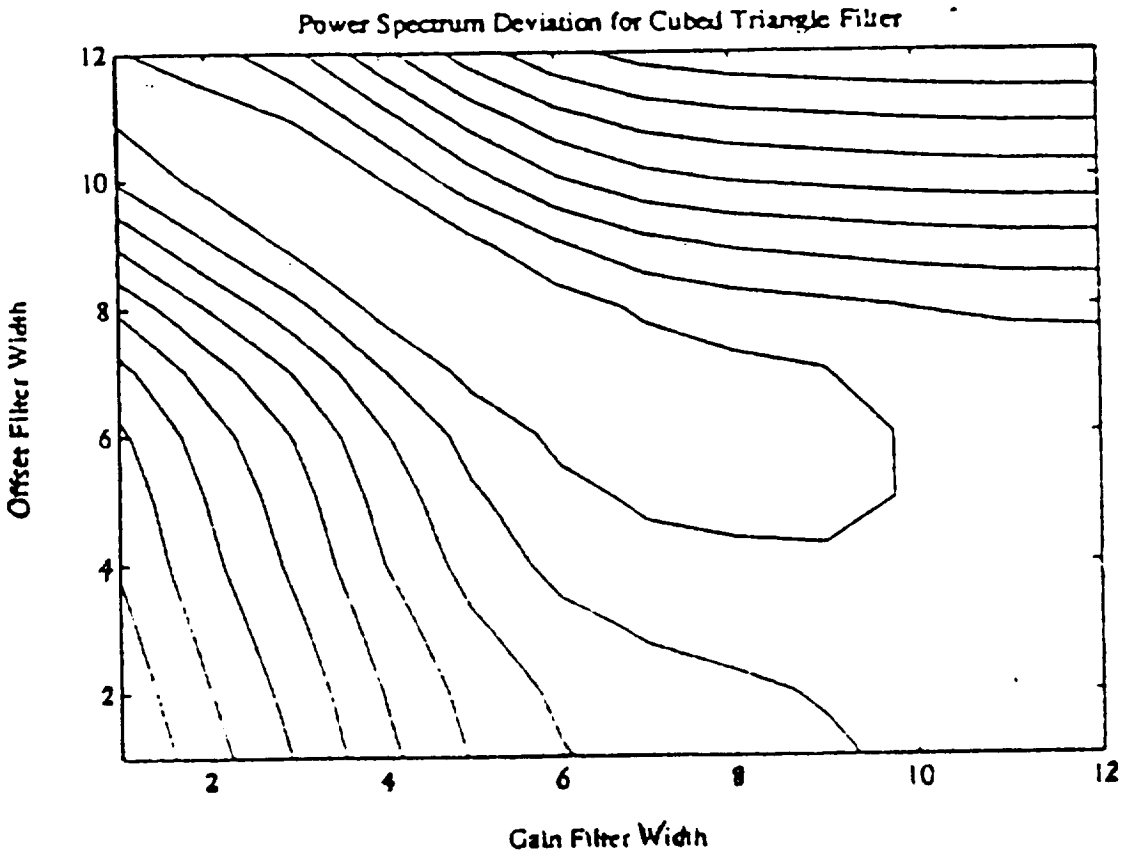

Figure 3. RMS noise contours for clear-air brightness data at 325+/-1 GHz as a function of the gain and offset filter widths. Contour intervals are approximately 1 K, with the lowest (center) contour being 7 K. The filter width scales are logarithmic, ranging from a width of unity to 2000.

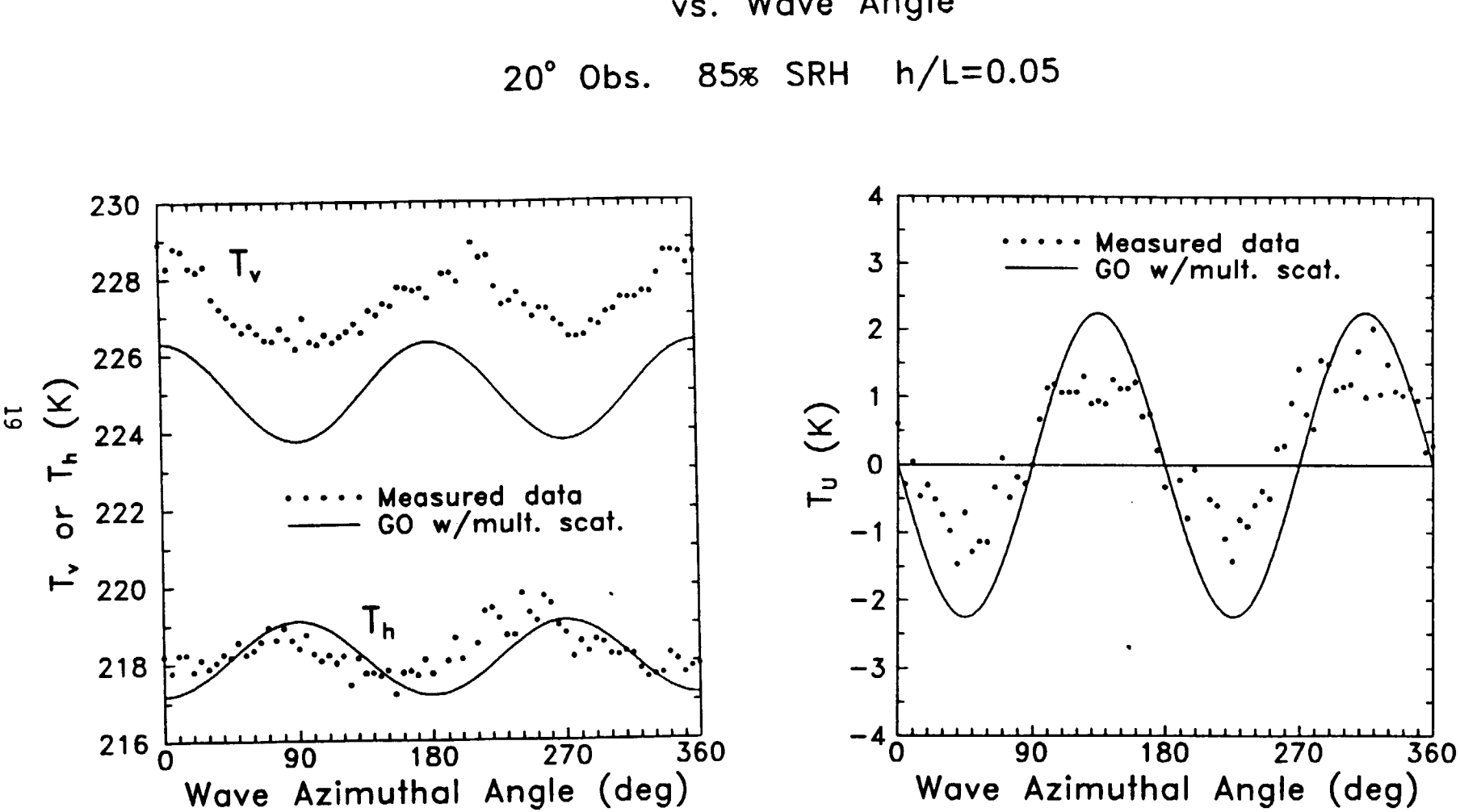

Figure 4. Measured and predicted brightness temperatures for T_V, T_h, and T_U as a function of azimuthal wave tank angle for the 92-GHz polarimetric laboratory measurements. The observation angle is 20^o from zenith.

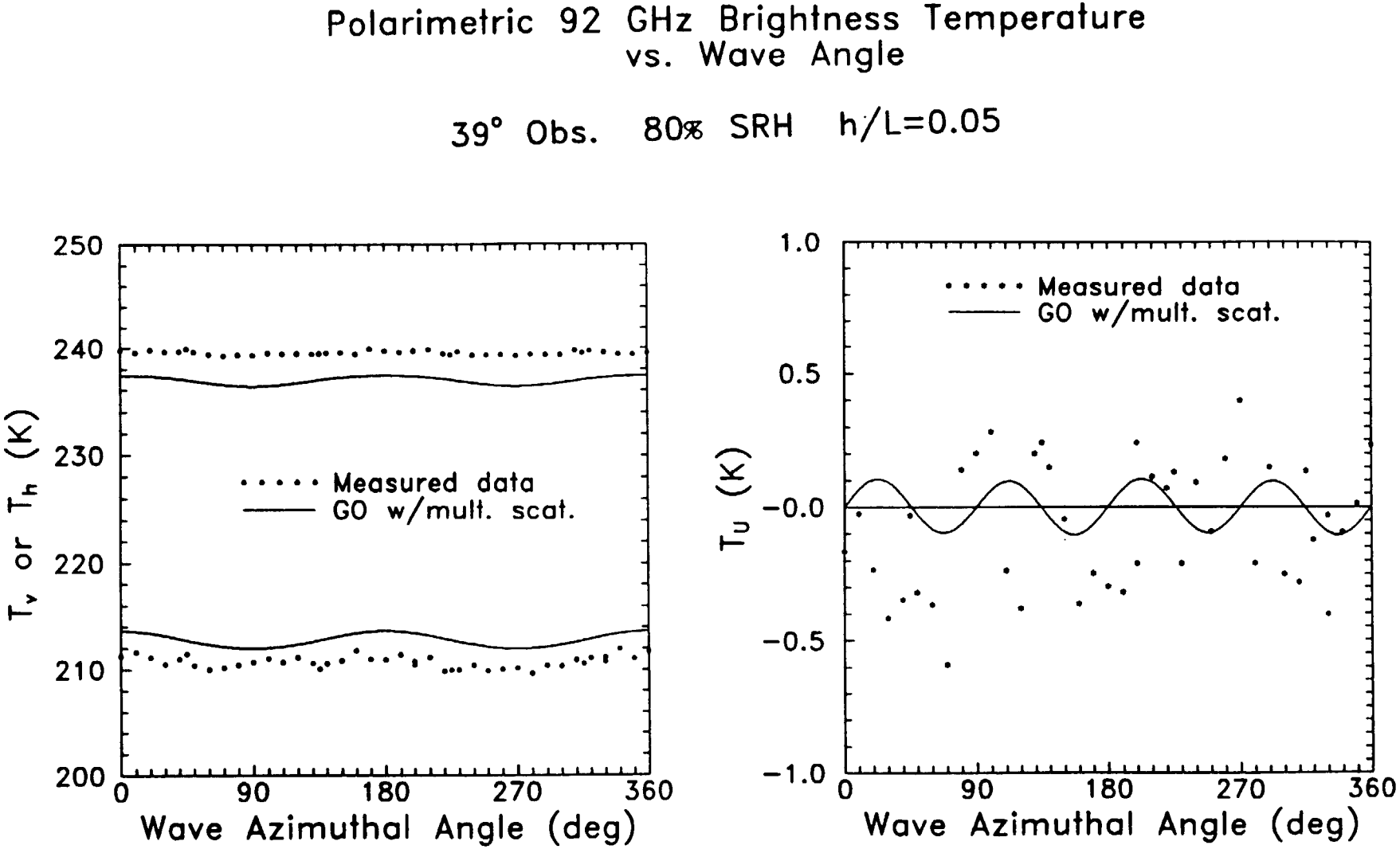

Figure 5. Measured and predicted brightness temperatures for T_v, T_h, and T_U as a function of azimuthal wave tank angle for the 92-GHz polarimetric laboratory measurements. The observation angle is 39° from zenith.

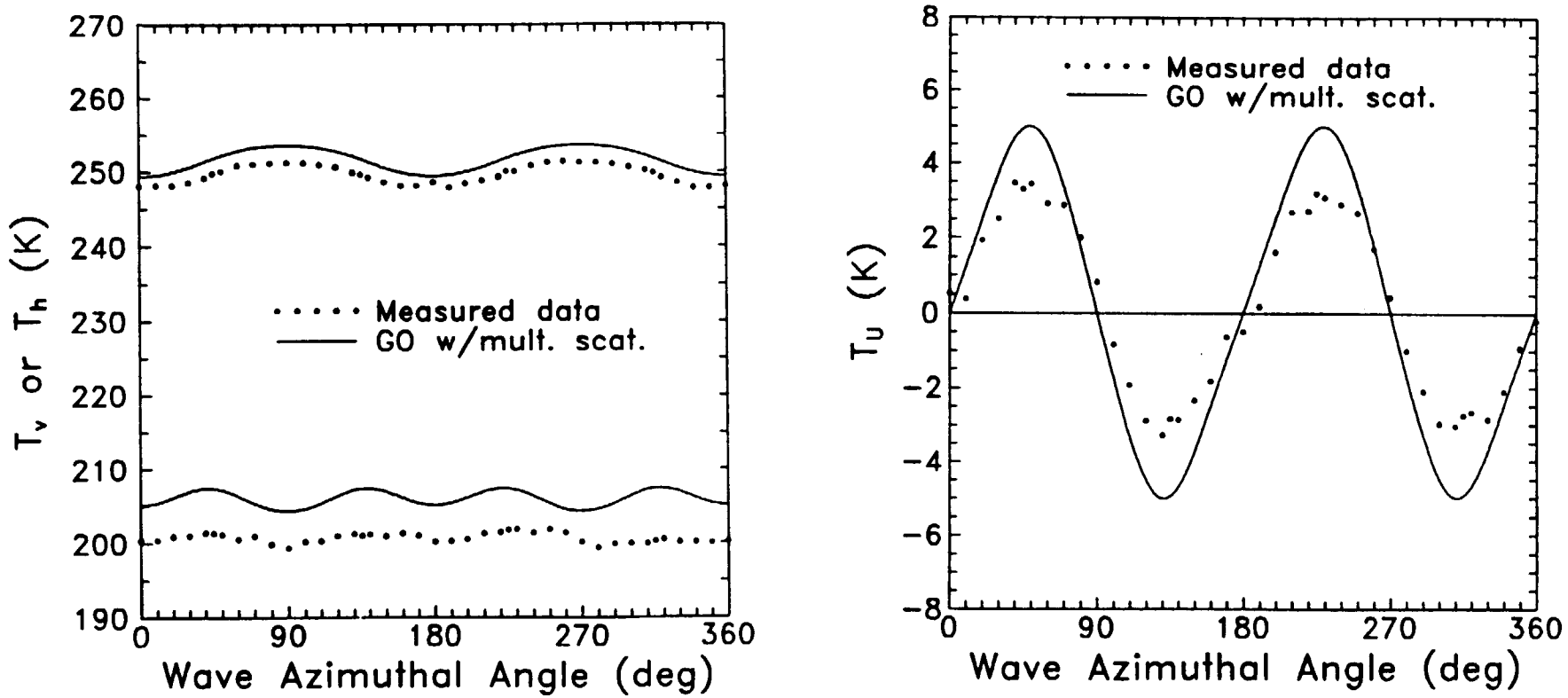

Figure 6. Measured and predicted brightness temperatures for T_V, T_h, and T_U as a function of azimuthal wave tank angle for the 92-GHz polarimetric laboratory measurements. The observation angle is 53° from zenith.

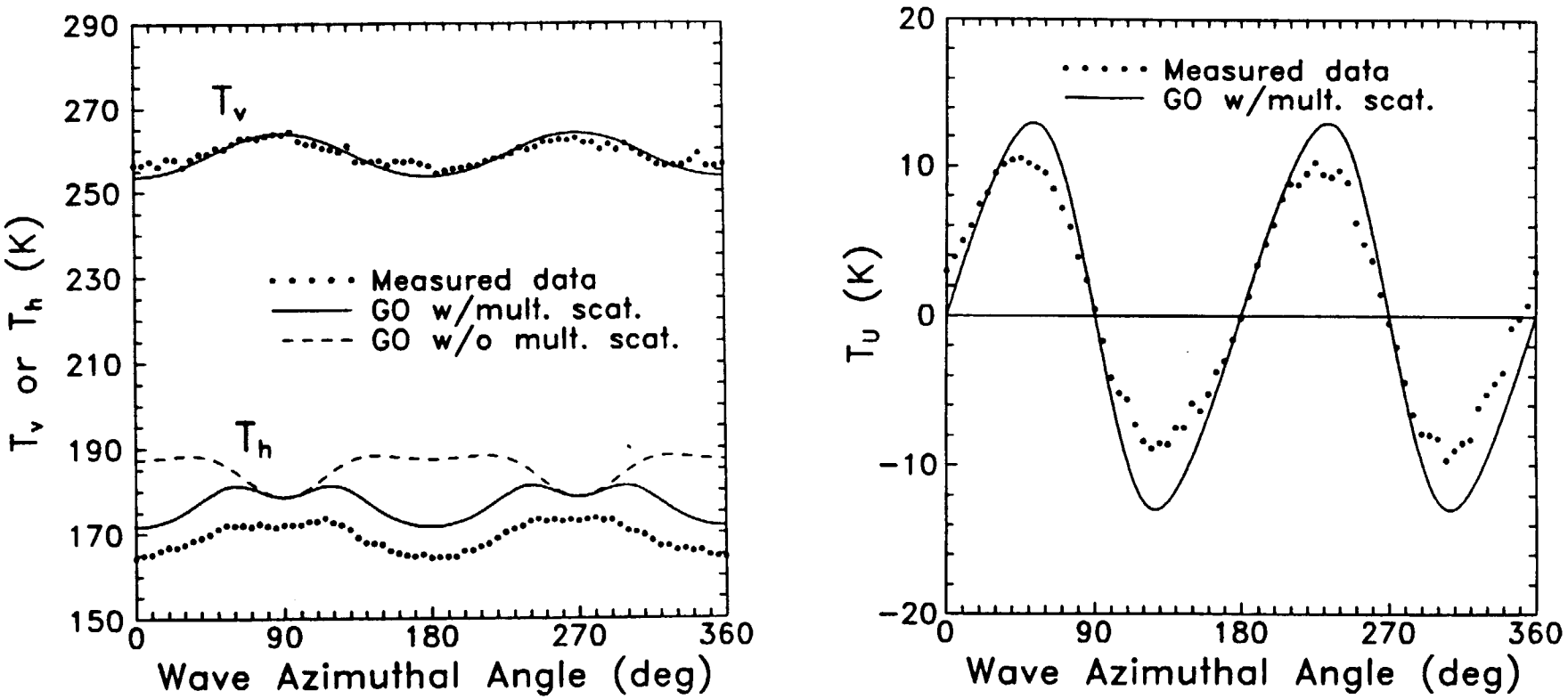

Figure 7. Measured and predicted brightness temperatures for T_V, T_h, and T_U as a function of azimuthal wave tank angle for the 92-GHz polarimetric laboratory measurements. The observation angle is 65° from zenith. The impact of neglecting multiple scattering is shown by the dashed line, and is significant only for T_h.

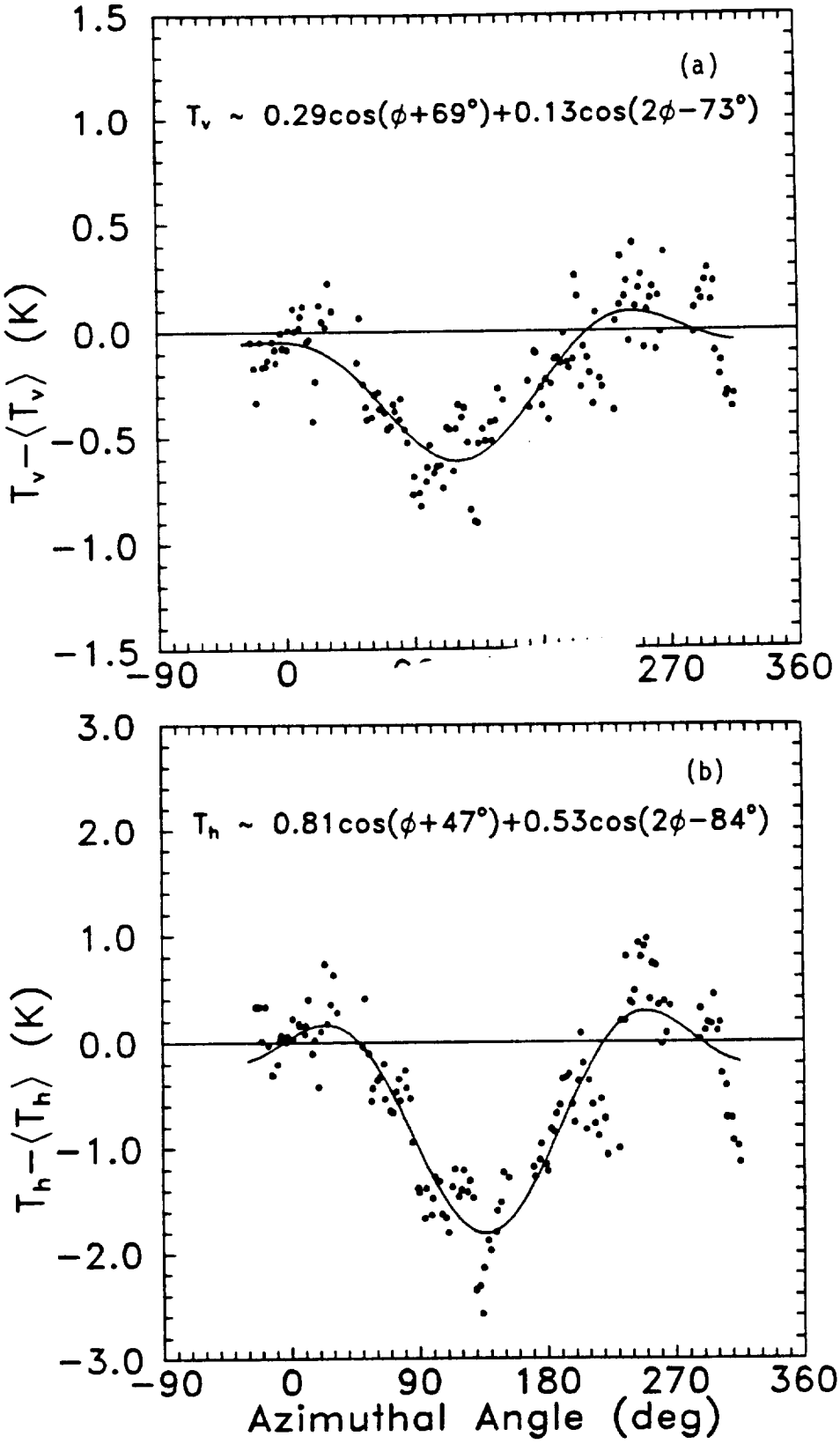

Figure 8. Measured azimuthal variation of T_V and T_h with wind direction observed at 91.65 GHz and an observation angle of 65° from nadir during TOGA/COARE. Conditions are light wind over open ocean.

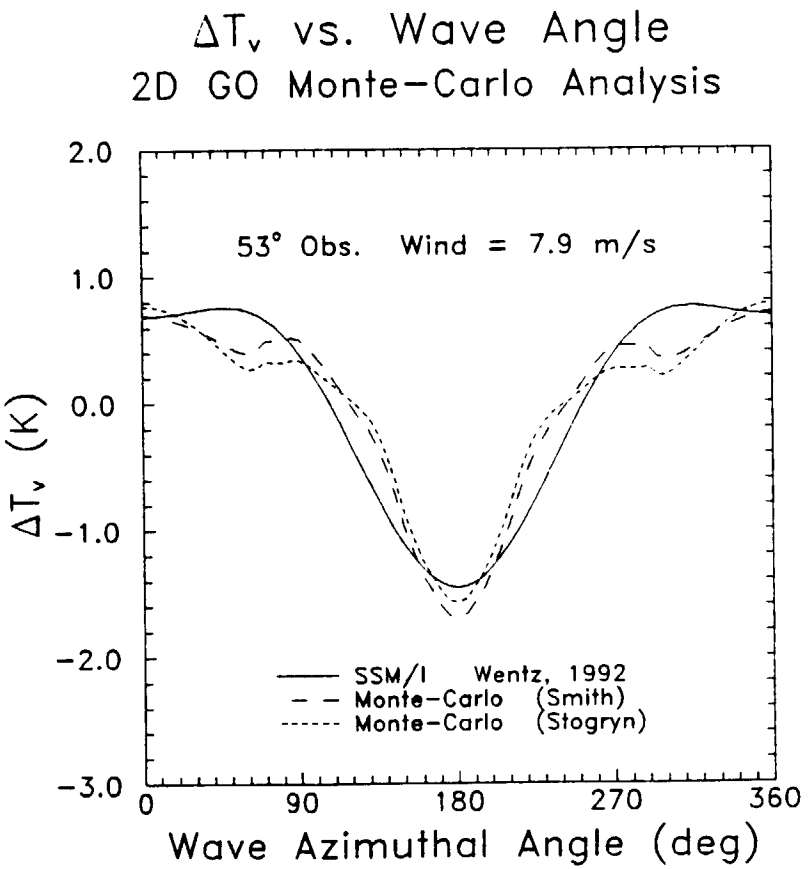

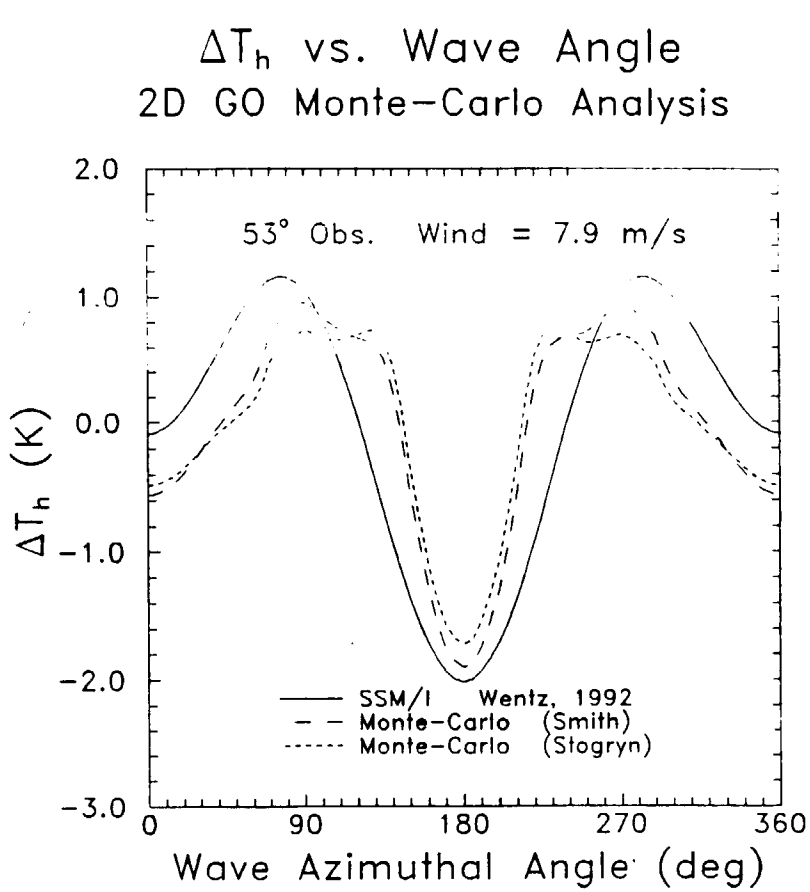

Figure 9. Comparison of azimuthal brightness variations computed using the geometrical optics scattering model applied to simulated ocean surfaces with the Wentz SSM/I data at 37 GHz. The statistical ocean surface model incorporates foam and statistical wave asymmetry.

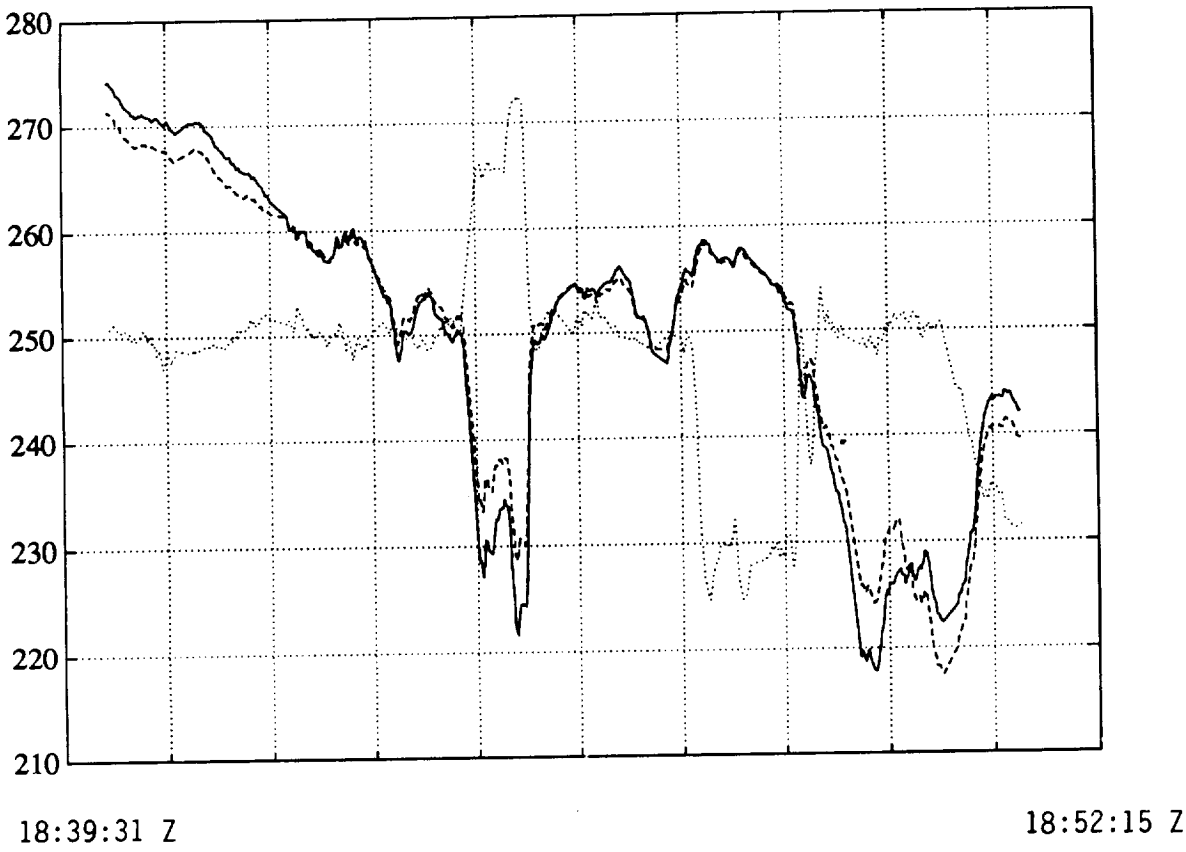

Figure 10. Vertical and horizontal brightness variations observed from the NSA DC-8 at 92-GHz during overflights of convection. The arrows point to rapid changes in the polarization difference that are not instrumental nor related to the aircraft roll. The polarization differences occurred over the most radiometrically cold portion of the storm.